

# Coherent-state process tomography of continuous-variable quantum gates

Simone Gasparinetti

Quantum Nanophotonics 2023  
Benasque, March 15

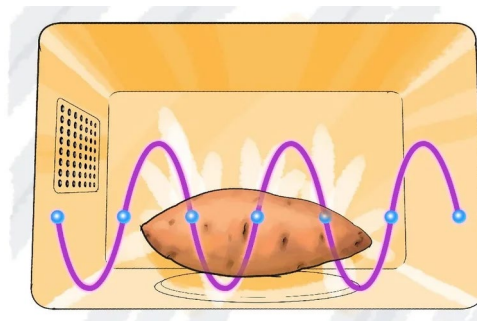
202Q·LAB



WACQT



# Preface: Quantum Optics vs Microwave Quantum Optics



Lasers and photodetectors

Optical fibers, integrated waveguides

Real or synthetic atoms

Quantum at room  $T$

Waveform generators and digitizers

Coaxial cables and waveguides

Synthetic atoms

Quantum at cryogenic  $T$

**Light-matter interactions described by same equations: Jaynes-Cummings and beyond**

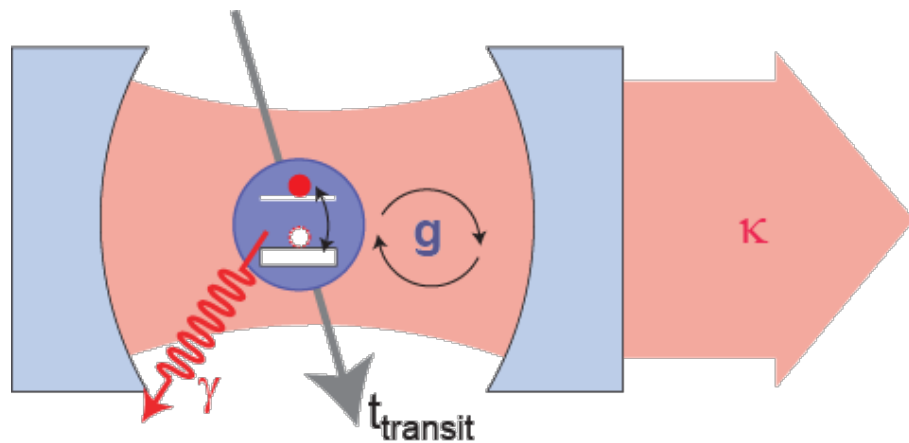
Some things are **EASY**

Some things are **HARD**

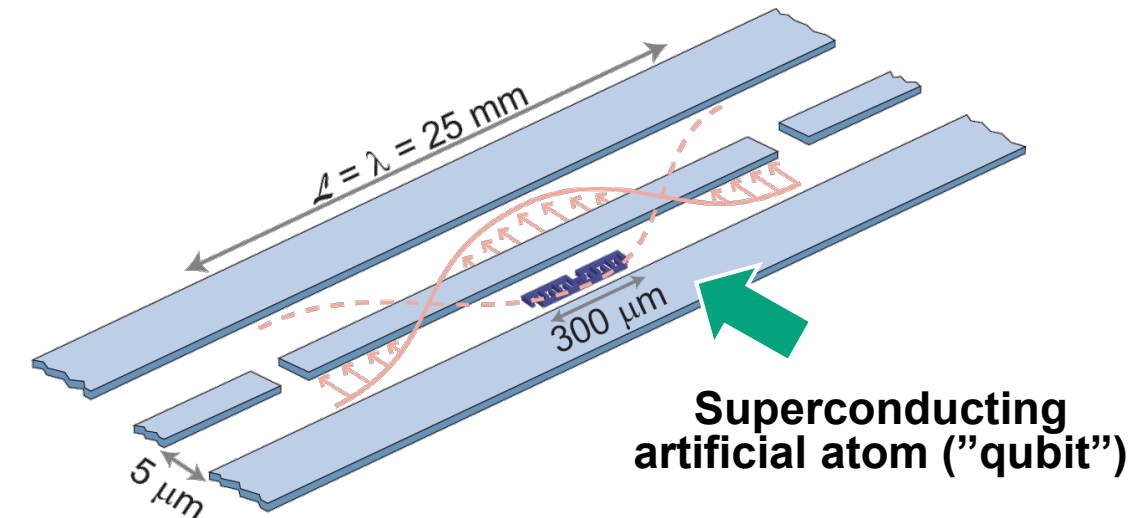
Some things are **HARD**

Some things are **EASY**

# From Cavity QED to Circuit QED



Raimond et al., Rev Mod Phys 73, 565 (2001)  
 Haroche & Raimond, OUP Oxford (2006)  
 Ye et al., Science 320, 1734 (2008)



Blais et al., Phys Rev A 69, 062320 (2004)  
 Wallraff et al., Nature 431, 162 (2004)  
 Schoelkopf & Girvin, Nature 451, 664 (2008)

**Quantum information processing (Google, IBM...)**  
**Microwave quantum optics**

# This talk

## Part I. Waveguide QED: project overview

- Symmetry-selective couplings
- Structured environments and atom-photon bound states
- Quantum thermodynamics with hot waveguides

## Part II. Coherent-state process tomography of a quantum gate

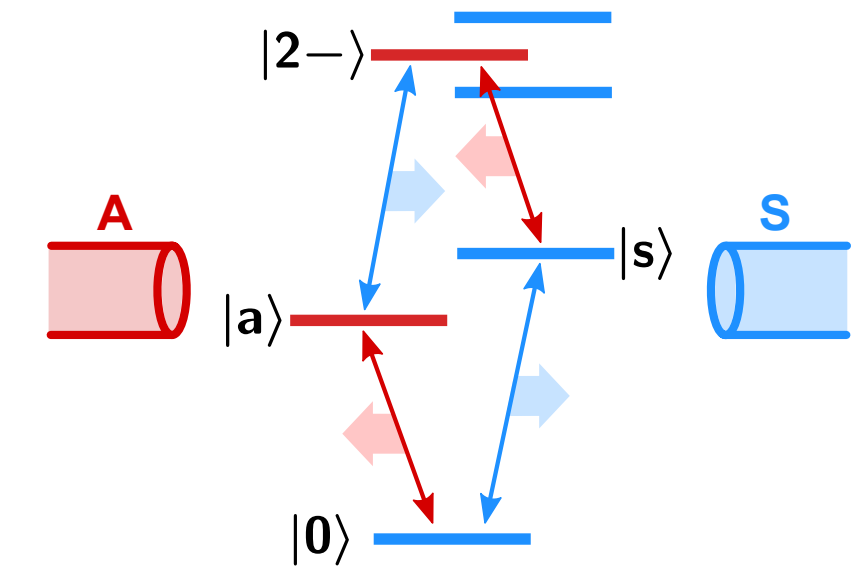
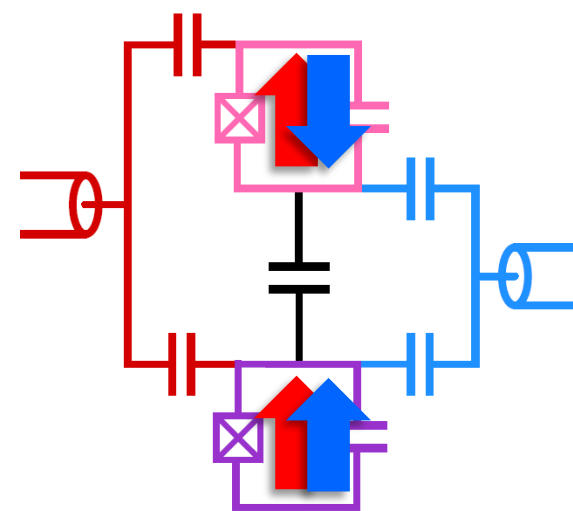
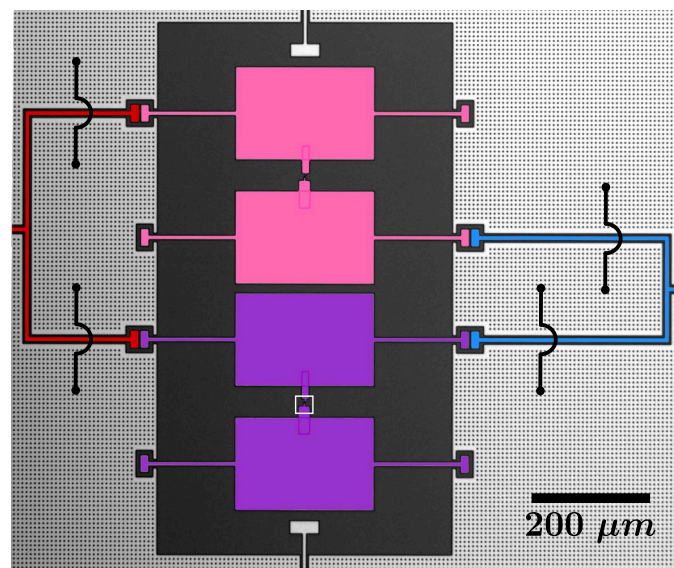
- Quantum computation with bosonic modes
- Deterministic preparation of nonclassical states
- X-gate on qubit encoded in a bosonic mode and its tomography

Wigner  
functions!

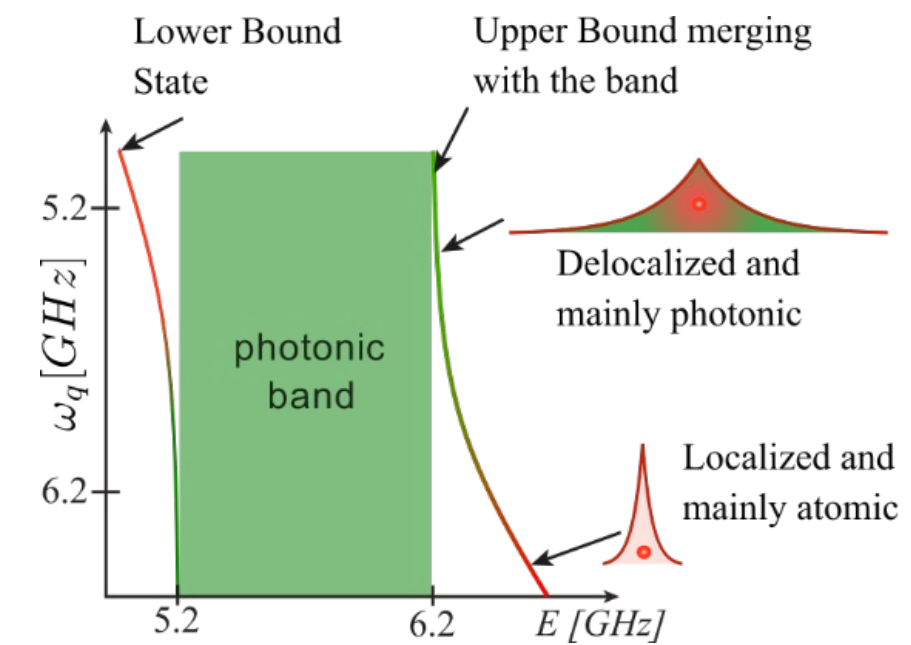
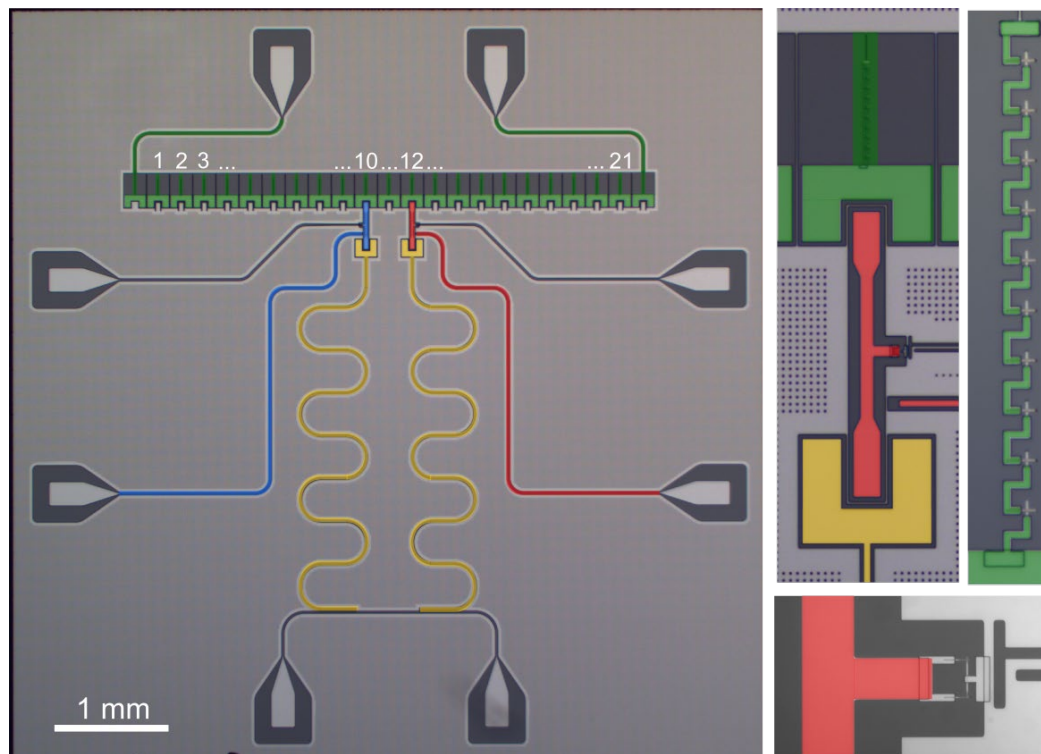
# Part I

202Q · LAB

# Symmetry-selective coupling of an artificial molecule to microwave waveguides

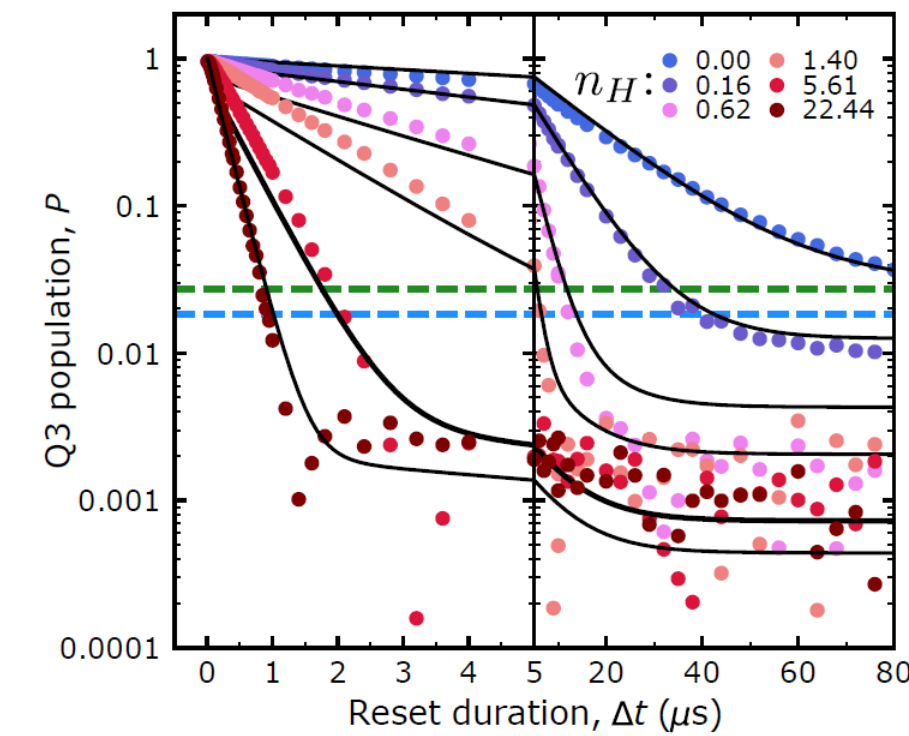
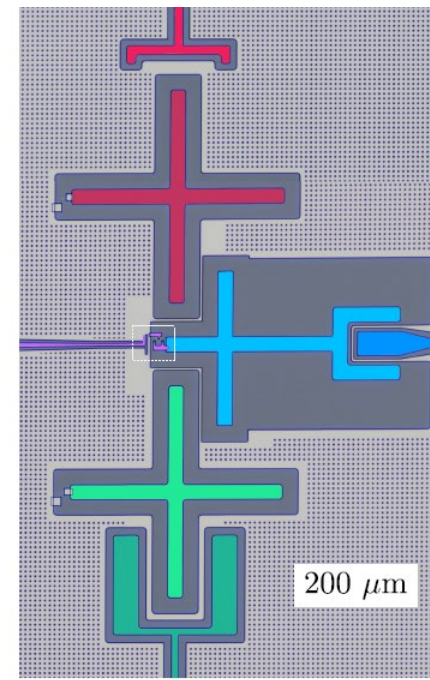
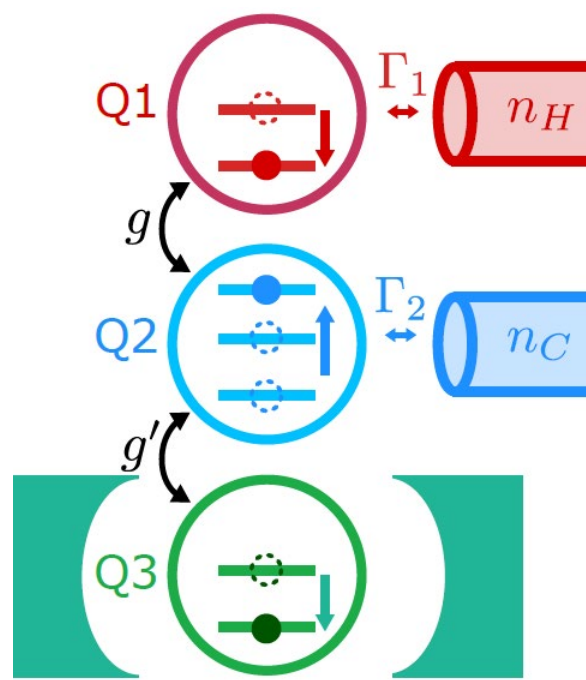


# Quantum emitters coupled to a structured environment: Atom-photon bound states and their interaction



# Quantum thermal machines coupled to waveguides

... Waveguide QTD?



# Part II

202Q · LAB

# Quantum computation with bosonic modes



High-quality Al microwave cavities

Kudra *et al.* *int Delsing*, *APL* **117**, 070601 (2020)

Microwave transceiver based on RFSoC

Tholén *et al.* *int Haviland*, *Rev. Sci. Instr.* **93**, 104711 (2022)

State preparation with SNAP-displacement sequences

Kudra *et al.* *int SG*, *PRX Quantum* **3**, 030301 (2022)

## Coherent-state quantum process tomography (experiment)

Mikael Kervinen, Marina Kudra, Shahnawaz Ahmed, Axel Eriksson, Fernando Quijandría, Anton Frisk Kockum, Per Delsing, and SG, [arXiv:2303.01451](https://arxiv.org/abs/2303.01451)

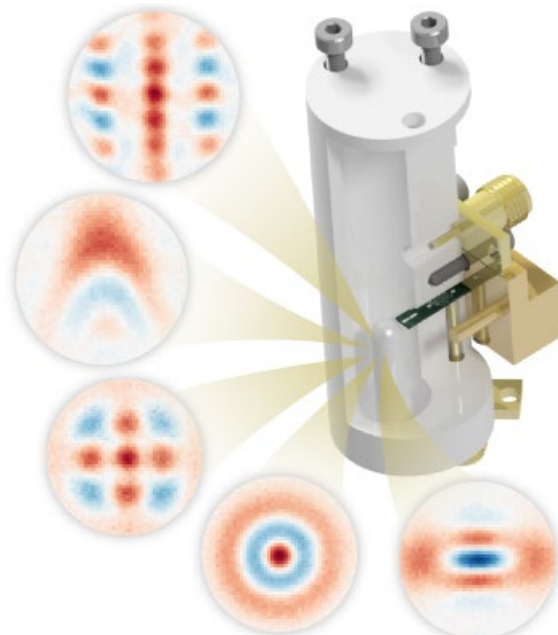


Gradient-Descent Quantum Process Tomography (theory)

Ahmed, Quijandría & Kockum, [arXiv:2208.00812](https://arxiv.org/abs/2208.00812)

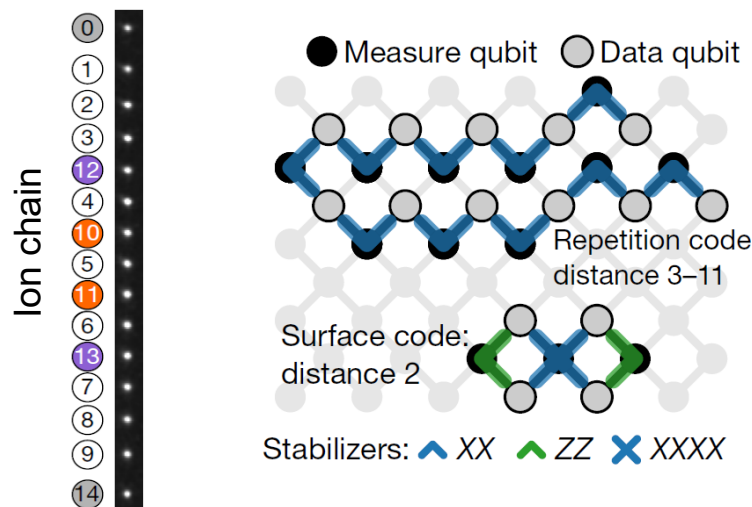
Selective photon addition for quantum error correction

Kudra *et al.* *int SG*, [arXiv:2212.12079](https://arxiv.org/abs/2212.12079)



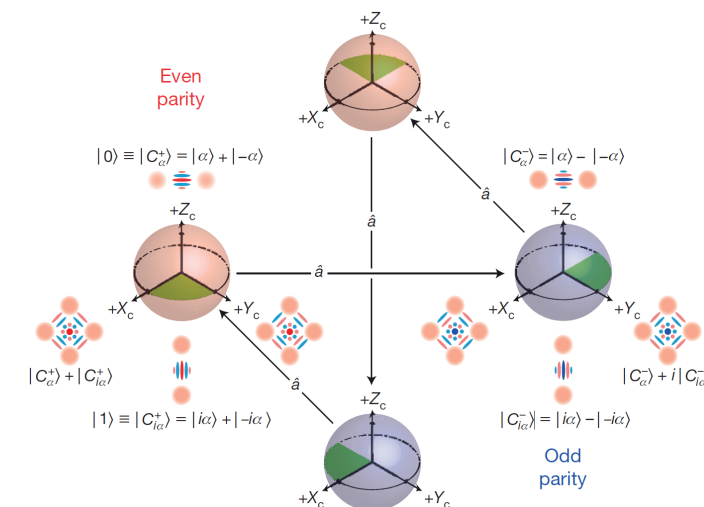
# Towards quantum error correction: logical qubits

## Multiple two-level systems



Andersen, et al, Wallraff, Nat Phys 16, 875 (2020)  
Marques, et al, DiCarlo, Nat Phys 18, 80 (2022)  
Google Quantum AI, Nature 595, 383 (2021)  
Krinner, et al, Wallraff, Nature 605, 669 (2022)  
Egan, et al, Monroe, Nature 598, 281 (2021)

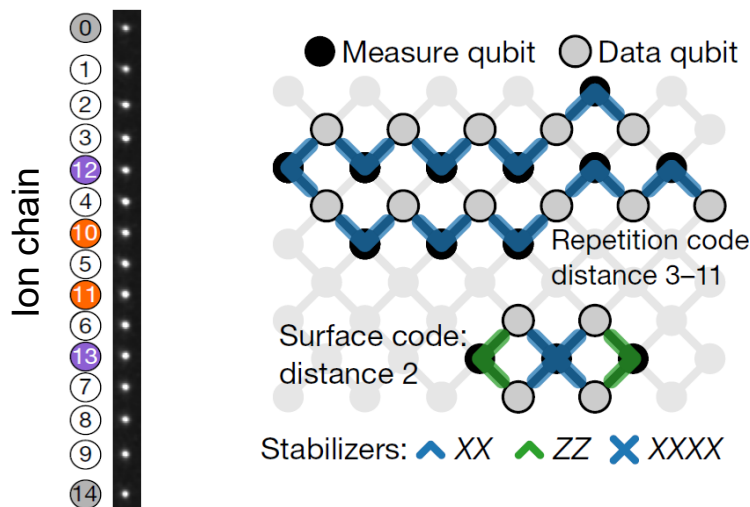
## Single harmonic oscillator



Ofek, et al, Schoelkopf, Nature 536, 441 (2016)  
Lescanne, et al, Leghtas, Nature Phys 16, 509 (2020)  
Grimm, et al, Devoret, Nature 584, 7820 (2020)  
Campagne-Ibarcq, et al, Devoret, Nature 584, 7821 (2020)  
Gertler, et al, Wang, Nature 590, 7845 (2021)

# Towards quantum error correction: logical qubits

## Multiple two-level systems



Andersen, et al., Wallraff, Nat Phys 16, 875 (2020)  
Marques, et al., DiCarlo, Nat Phys 18, 80 (2022)  
Google Quantum AI, Nature 595, 383 (2021)  
Krinner, et al., Wallraff, Nature 605, 669 (2022)  
Egan, et al., Monroe, Nature 598, 281 (2021)

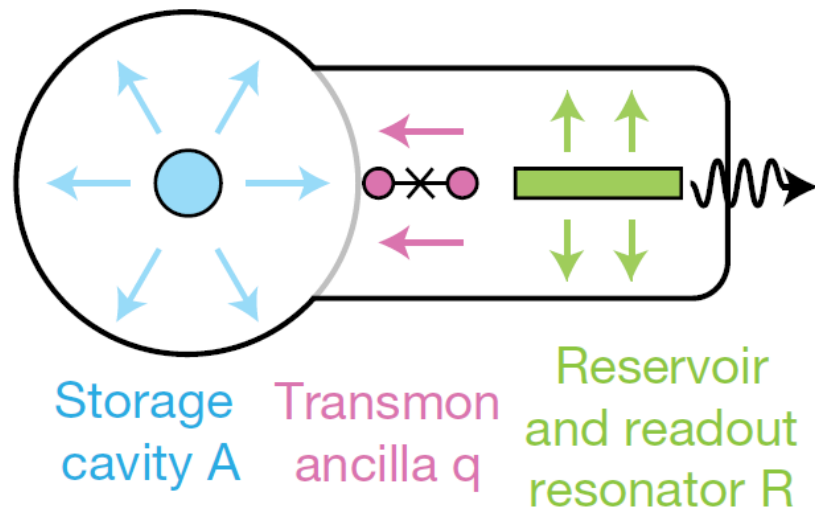
## Single harmonic oscillator

Resource-efficient  
Long coherence times  
One dominant error mechanism

Control? Needs nonlinearity

Ofek, et al., Schoelkopf, Nature 536, 441 (2016)  
Lescanne, et al., Leghtas, Nature Phys 16, 509 (2020)  
Grimm, et al., Devoret, Nature 584, 7820 (2020)  
Campagne-Ibarcq, et al., Devoret, Nature 584, 7821 (2020)  
Gertler, et al., Wang, Nature 590, 7845 (2021)

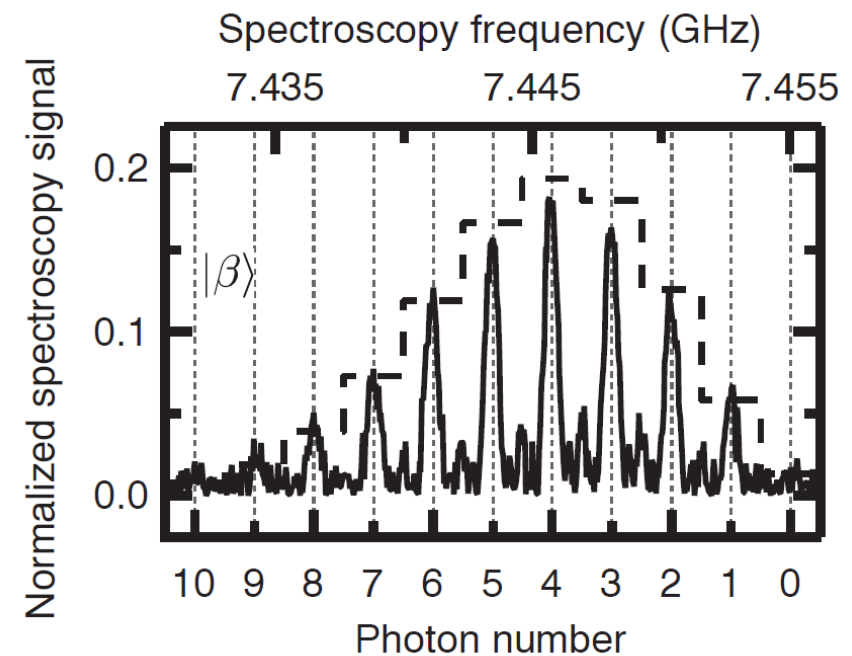
# Harmonic oscillator + ancillary qubit = universal control



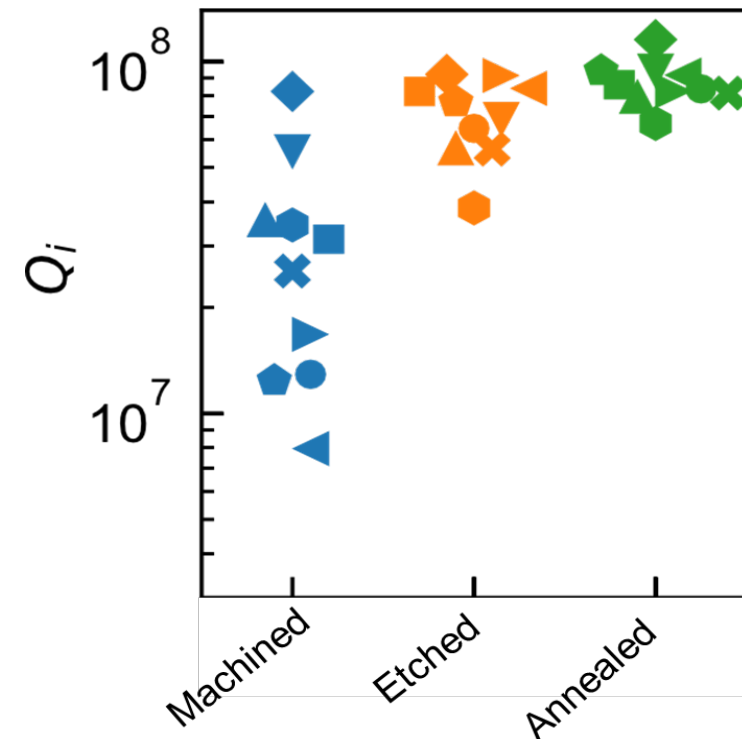
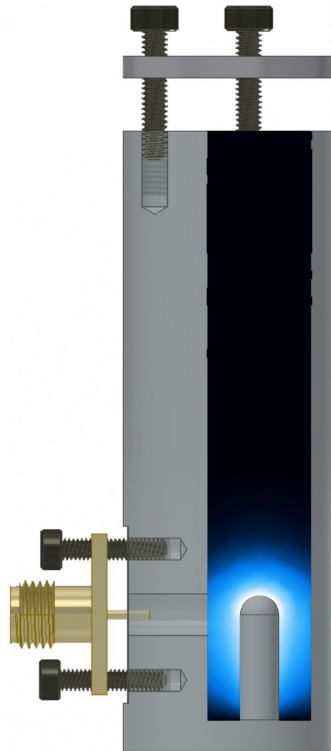
Gertler, et al., Wang, Nature 590, 7845 (2021)  
Vlastakis et al., Schoelkopf, Science 342, 6158 (2013)  
Krastanov et al., Jiang, PRA 92, 040303 (2015)  
Heeres et al., Schoelkopf, PRL 115, 137002 (2015)  
--- Nat Commun 8, 94 (2017)  
Eickbusch et al., Devoret, Nat Phys 18, 1464 (2022)

## Strong dispersive regime

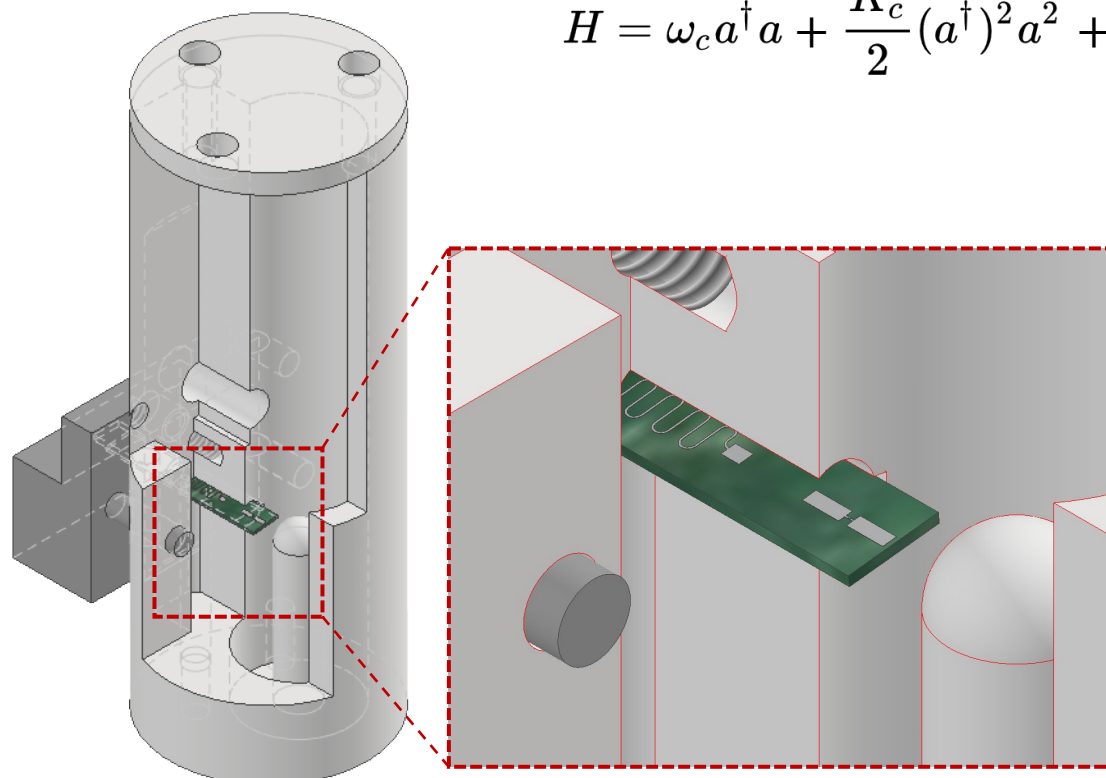
$$H = \omega_r a^\dagger a + \omega_q b^\dagger b + \chi a^\dagger a b^\dagger b$$



# Quantum memory: 3D aluminum cavity



# Transmon coupled to 3D cavity



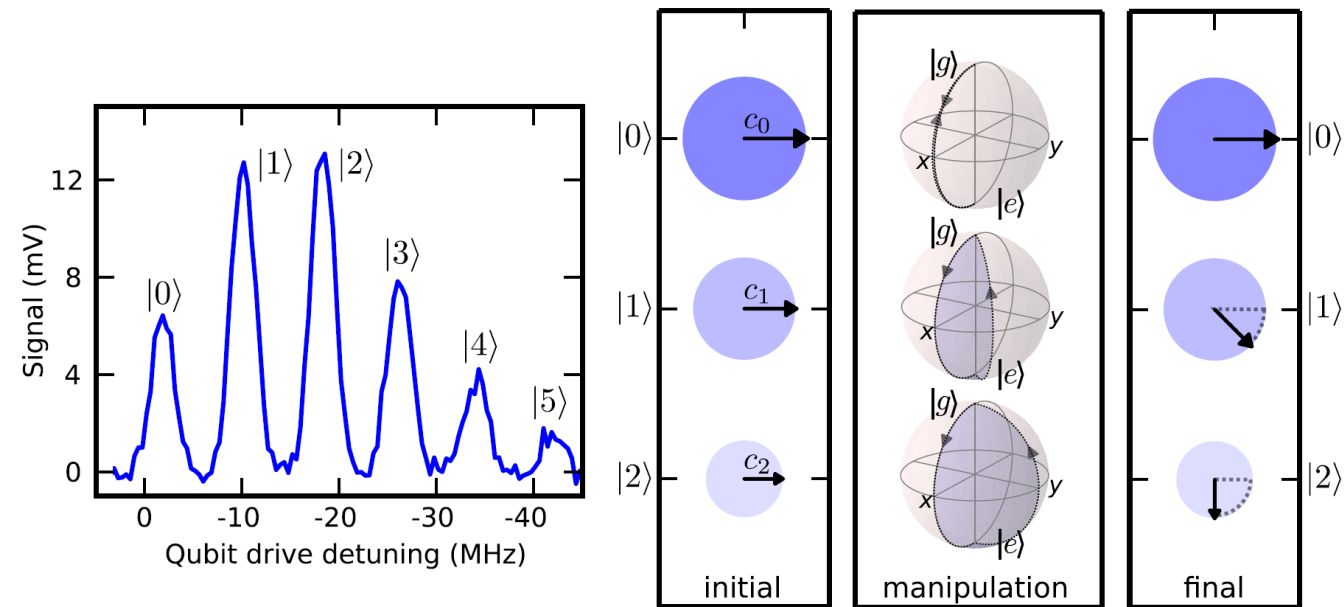
$$H = \omega_c a^\dagger a + \frac{K_c}{2} (a^\dagger)^2 a^2 + \omega_q b^\dagger b + \chi_{qc} a^\dagger a b^\dagger b + \chi'_{qc} (a^\dagger)^2 a^2 b^\dagger b$$

Parameter	Symbol	Value
Transmon frequency	$\omega_q/2\pi$	6.281 GHz
Cavity frequency	$\omega_c/2\pi$	4.454 GHz
Readout resonator frequency	$\omega_r/2\pi$	7.348 GHz
Transmon-cavity cross-Kerr	$\chi_{qc}/2\pi$	-2.22 MHz
Transmon-resonator cross-Kerr	$\chi_{qr}/2\pi$	-1.4 MHz
Cavity self-Kerr	$K_c/2\pi$	-2.7 kHz
Transmon anharmonicity	$\alpha_q/2\pi$	-353 MHz
Transmon-cavity higher-order cross-Kerr.	$\chi'_{qc}/2\pi$	-14 kHz
Transmon energy decay time	$T_{1q}$	$\approx 38 \mu\text{s}$
Transmon pure dephasing time	$T_{\Phi q}$	$\approx 127 \mu\text{s}$
Cavity decay time	$T_{1c}$	$\approx 315 \mu\text{s}$
Transmon thermal population	$\bar{n}_q$	0.005
Cavity thermal population	$\bar{n}_c$	0.003

# Selective Number-dependent Arbitrary phase (SNAP) gates

$$S(\vec{\theta}): \sum c_n |n\rangle \otimes |g\rangle \rightarrow \sum c_n e^{i\theta_n} |n\rangle \otimes |g\rangle$$

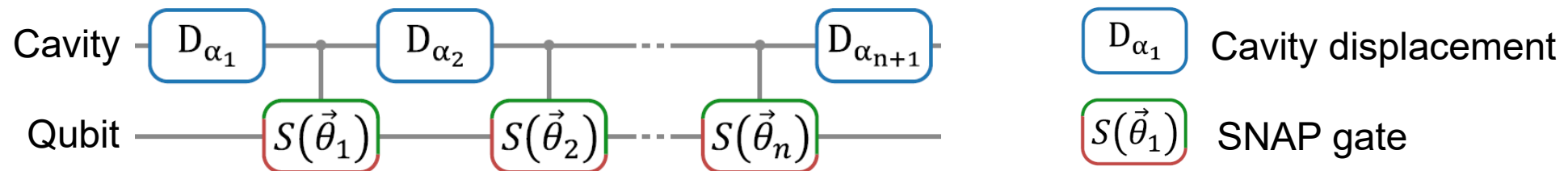
**How do we do it?  
I will explain**



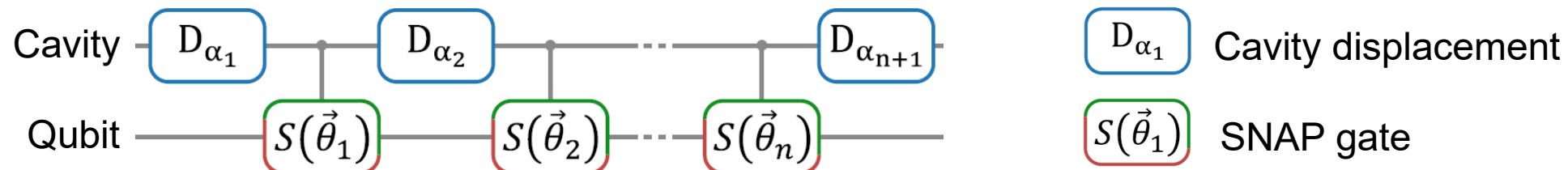
**SNAP + Displacements = Universal control  
How efficient?**

Heeres *et int* Schoelkopf, PRL 115, 137002 (2015)  
Krastanov *et int* Jiang, PRA 92, 040303 (2015)  
Fösel *et int* Jiang, ArXiv:2004.14256  
Kudra *et int* SG, PRX Quantum 3, 030301 (2022)

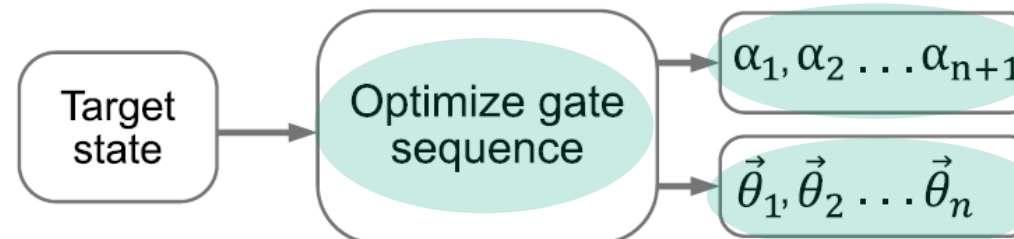
## Two-step optimization of SNAP gate sequences



# Two-step optimization of SNAP gate sequences



1



Gradient-based optimization of fidelity to target state

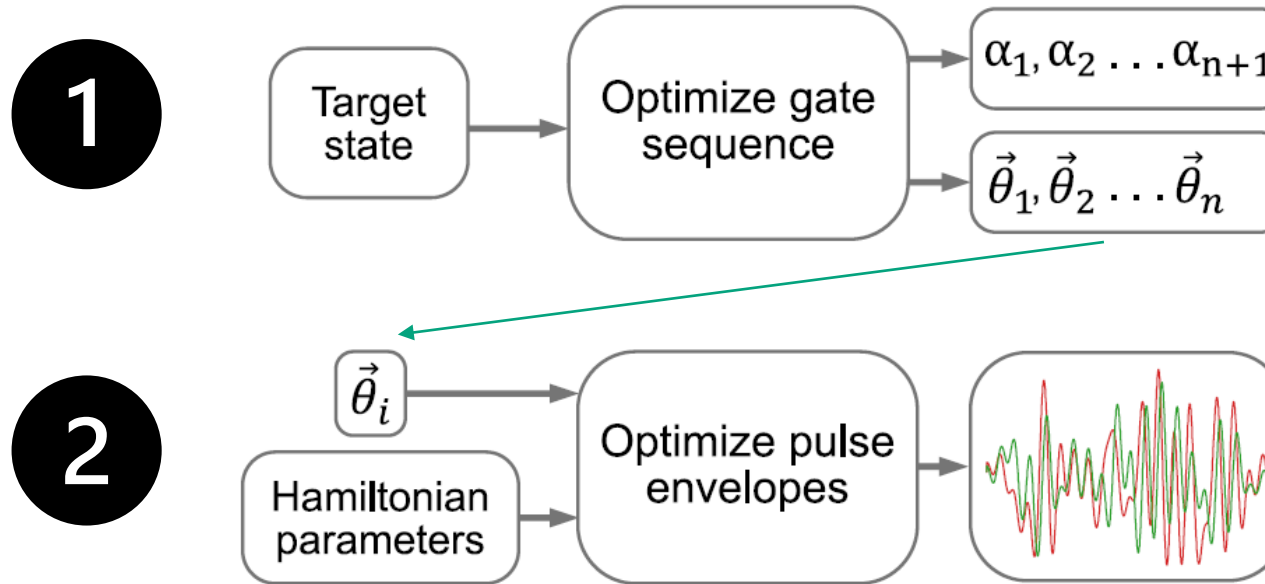
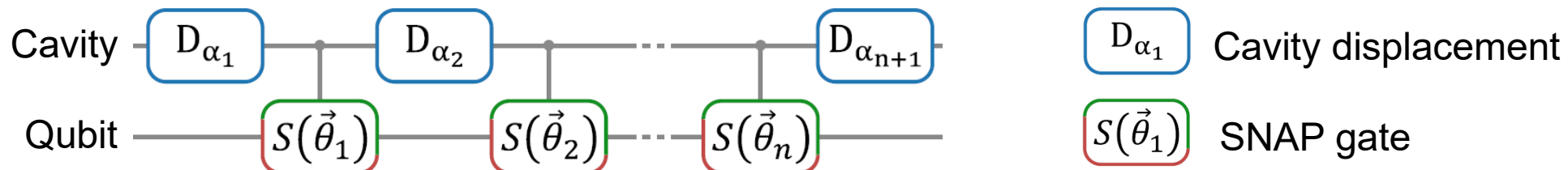
Amplitudes of displacement pulses

Phases to impart to Fock states

$m$ : largest targeted Fock state    **Up to  $m = 17$ !**

$$\vec{\theta}_i = (\theta_{i,0}, \theta_{i,1}, \dots, \theta_{i,m})$$

# Two-step optimization of SNAP gate sequences



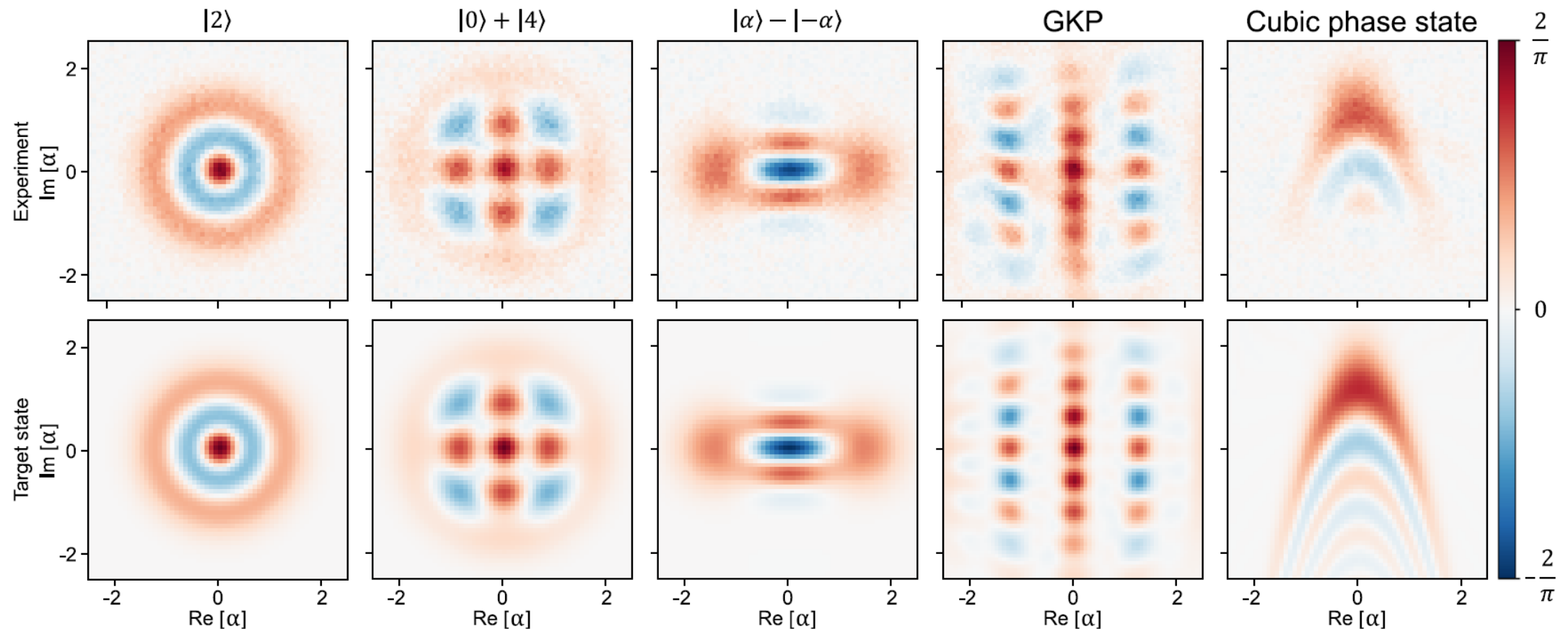
From calibration measurements<sup>1</sup>



Q-CTRL

<sup>1</sup> P. Reinhold, Ph.D. thesis, Yale Univ. (2019)

# Some states we can generate with SNAP+displacements



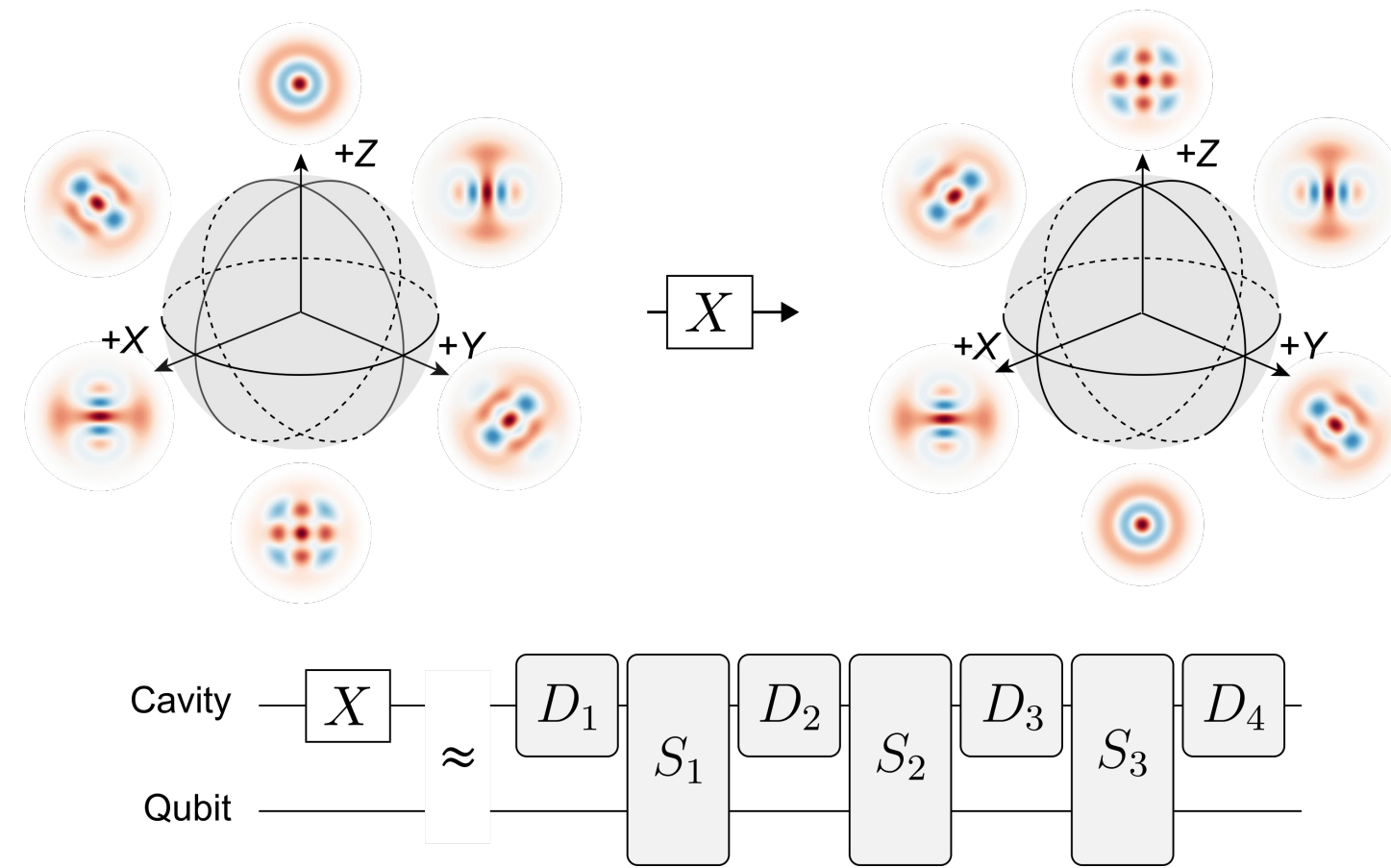
# From states to gates: X-gate in binomial encoding

**Binomial encoding**

$$|0_L\rangle = |2\rangle$$

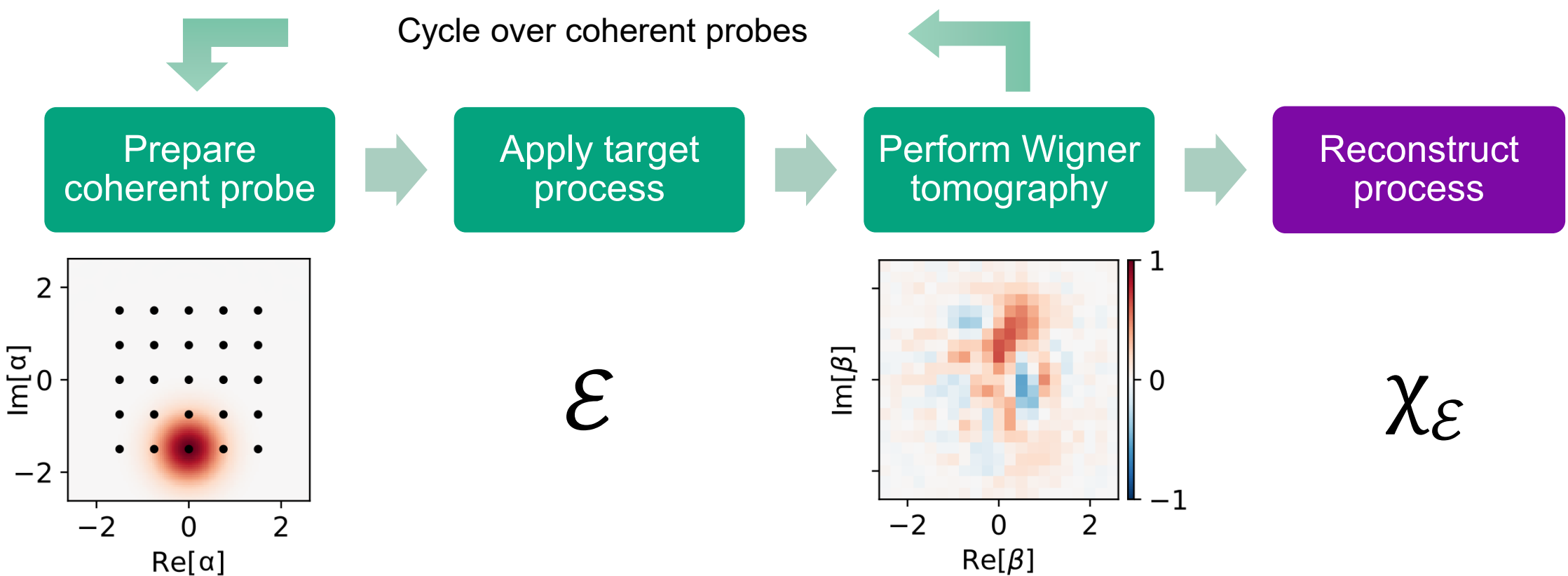
$$|1_L\rangle = |0\rangle + |4\rangle$$

**Gate decomposition**  
Ideal fidelity: 99.6%

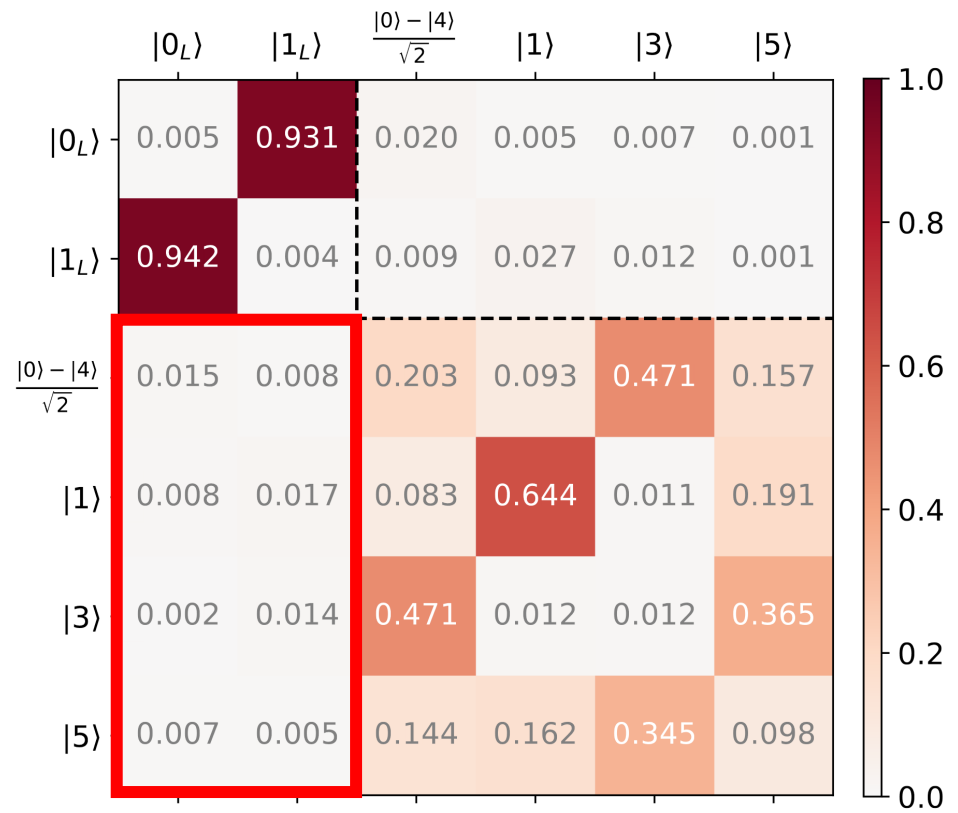


**But how to characterize the gate?**

# Coherent-state quantum process tomography (csQPT)



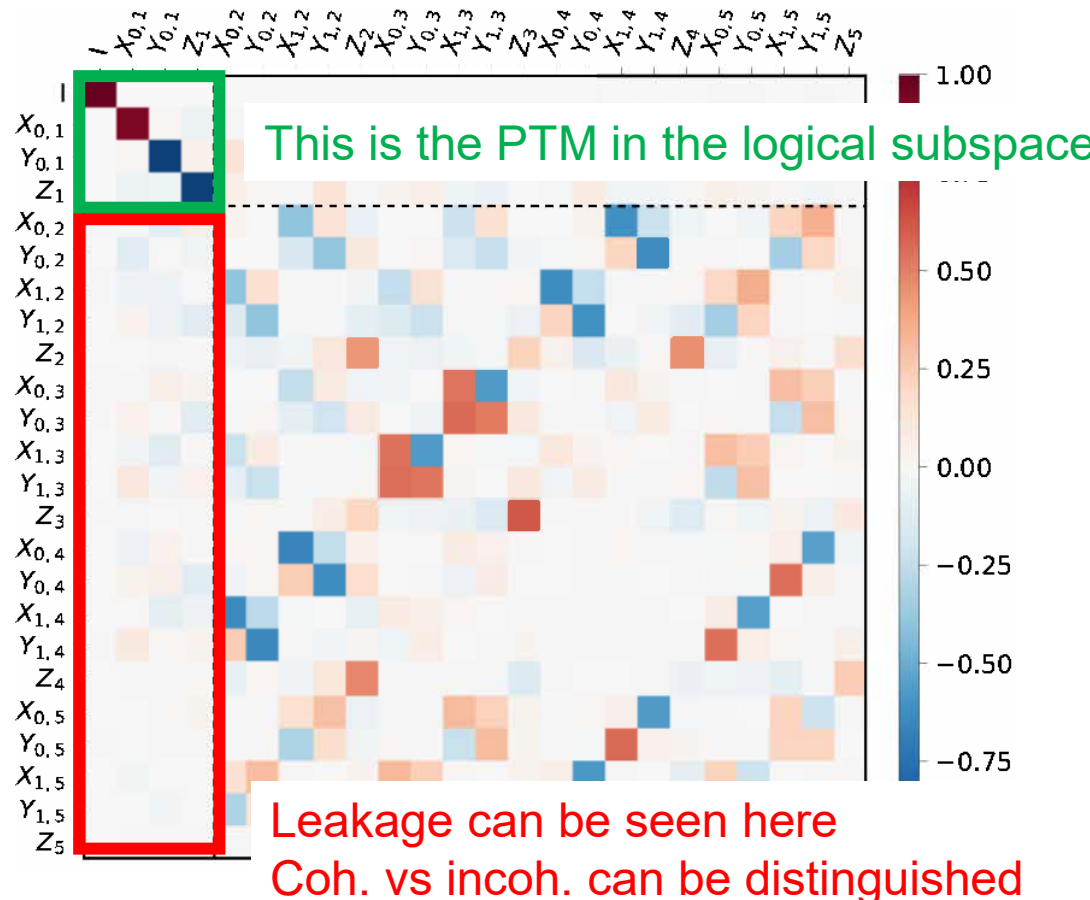
# Results: population transfer matrix



Leakage can be seen here

- Truncated up to the first 6 Fock states
- The logical basis is completed to span the truncated Hilbert space
- Visualizes population transfer within and outside of computational subspace
- Can be used to detect leakage
- Does not provide full information on the process

# Results: Generalized Pauli transfer matrix (“Gell-Mann transfer matrix”)



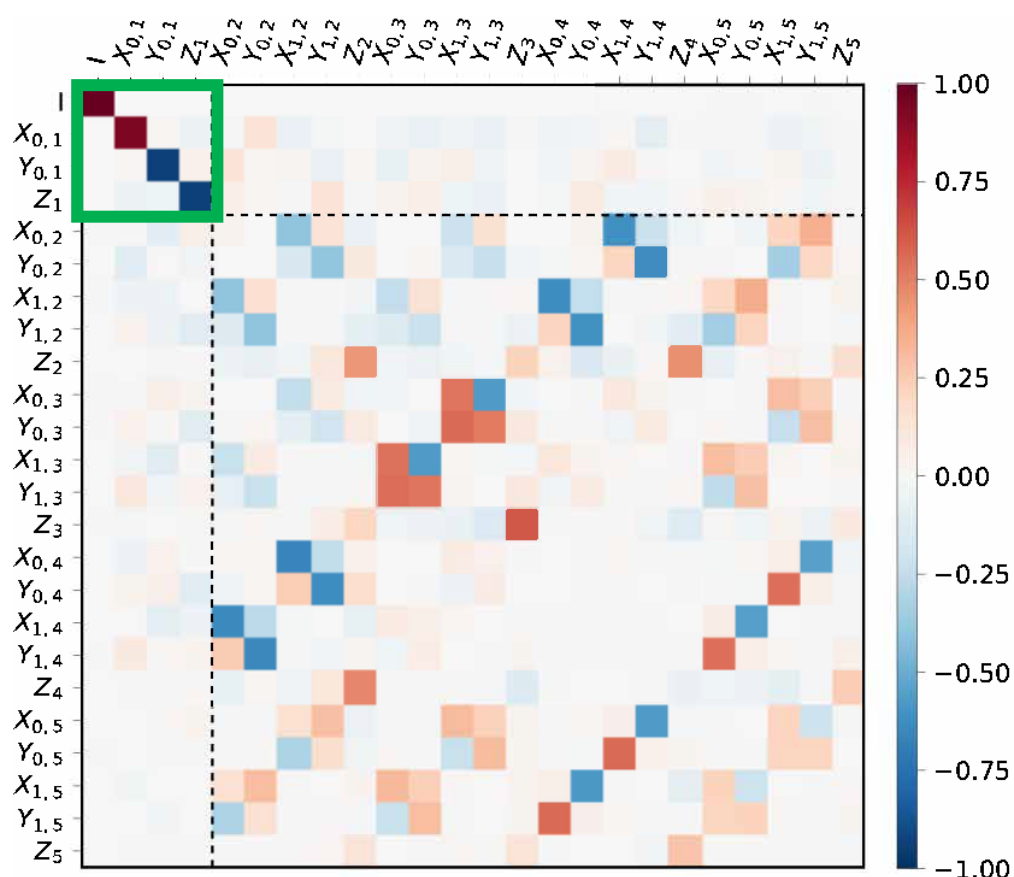
**Gell-Mann matrices.** A collection of Hermitian, traceless, orthonormal matrices  $\{G_i\}$  forming an operator basis for  $SU(N)$ . Generalize Pauli matrices for  $N > 2$ .

**Gell-Mann transfer matrix (GMTM).** A matrix representation of a process  $\mathcal{E}$  on a  $d$ -dimensional Hilbert space, defined as  $GMTM_{ij} = \text{Tr}[G_i \mathcal{E}(G_j)]$ . Generalize Pauli transfer matrix (PTM).

We arranged Gell-Mann matrices so that the top left block is the Pauli transfer matrix in the logical subspace.

We are only showing Gell-Mann matrices that couple to the logical subspace

# Results: Generalized Pauli transfer matrix (“Gell-Mann transfer matrix”)



	$I$	$X$	$Y$	$Z$
$I$	1.00	-0.00	-0.00	0.00
$X$	0.00	0.94	0.01	-0.05
$Y$	0.00	0.01	-0.94	0.04
$Z$	0.00	-0.05	-0.04	-0.93

exp      sim      ideal

Reduced Pauli transfer matrix agrees within 1% with simulation incl. qubit and cavity loss

Gate fidelity:

- Measured: 96.8%
- Simulated: 96.4%
- Ideal: 99.6%

# Advantages of coherent-state process tomography

Our implementation of csQPT:

- Requires **no encoding / decoding operations**, only displacements (most trusted operation)
- Returns **full process matrix** in the extended Hilbert space
- Uses a novel **gradient-descent-based optimization algorithm** to learn the Kraus representation of the process



Reduces SPAM errors



Detect leakage errors



Efficient reconstruction from a reduced number of data points

# Thank you!

## 202Q·LAB



WACQT



myfab

Knut and Alice  
Wallenberg  
Foundation



Swedish  
Research  
Council



European  
Innovation  
Council



More questions? [simoneq@chalmers.se](mailto:simoneq@chalmers.se)  
Visit our website [202q-lab.se](http://202q-lab.se)

